

m^* in InP to be larger than that in GaAs, the ratio being 1.04 compared to our ratio (see Ref. 4) of 1.09 (private communication).

⁶³C. Hilsum, S. Fray, and C. Smith, *Solid State Commun.* **7**, 1057 (1969).

⁶⁴L. Kleinman, *Phys. Rev.* **128**, 2614 (1962).

⁶⁵O. G. Folberth and H. Weiss, *Z. Naturforsch.* **10a**, 615 (1955).

⁶⁶V. V. Galavanov and N. V. Siukaev, *Phys. Status Solidi* **38**, 523 (1970).

⁶⁷L. W. James, J. P. VanDyke, F. Herman, and D. M. Chang, *Phys. Rev. B* **1**, 3998 (1970).

⁶⁸F. J. Reid and R. K. Willardson, *J. Electron.* **5**, 54 (1958).

⁶⁹M. Glicksman and K. Weiser, *J. Electrochem. Soc.* **105**, 728 (1958).

⁷⁰T. C. Harman, J. I. Genco, W. P. Allred, and H. L. Goering, *J. Electrochem. Soc.* **105**, 731 (1958).

⁷¹F. P. Kesamanly, D. N. Nasledov, A. Ya. Nashel'skii, and V. A. Skripkin, *Fiz. Zekh. Poluprov.* **2**, 1463 (1968) [*Sov. Phys. Semicond.* **2**, 1221 (1969)].

⁷²O. Roder, thesis (Goethe University, Frankfurt, 1969) (unpublished); O. Roder, U. Heim, and M. H. Pilkuhn, *J. Phys. Chem. Solids* (to be published).

⁷³M. Glicksman, *J. Phys. Chem. Solids* **8**, 511 (1959).

⁷⁴I. Kudman and E. F. Steigmeier, *Phys. Rev.* **133**, A1665 (1964).

⁷⁵G. G. Kovalevskaya and S. V. Slobodchikov, *Phys. Status Solidi* **30**, 441 (1968).

⁷⁶D. Richman, in Ref. 54, p. 214.

⁷⁷R. C. Clarke, B. D. Joyce, and W. H. E. Wilgoss, *Solid State Commun.* **8**, 1125 (1970).

⁷⁸Earlier data from various sources compiled in Ref. 71.

Coulomb Effects at Saddle-Type Critical Points in CdTe, ZnTe, ZnSe, and HgTe

Y. Pétroff and M. Balkanski

*Laboratoire de Physique des Solides de la Faculté des Sciences de Paris
Equipe de Recherche, associée au Centre National de la Recherche Scientifique
Paris, France*

(Received 13 October 1970)

The Kane model for saddle-point excitons is applied to CdTe, ZnTe, ZnSe, and HgTe by studying the shape of the imaginary part of the dielectric constant ϵ_2 obtained by reflectivity measurements at 10°K. We have obtained $|m_3/m_1| = 28$ for CdTe and 20 for ZnTe but we have not been able to measure the ratio for ZnSe or HgTe.

The effect of the interaction between electron and hole at an M_1 critical point is a very controversial problem.¹ An experimental approach² to this problem was suggested several years ago by Cardona and Harbeke. In the last few years, several theoreticians³⁻⁵ have treated the subject, but the first complete calculation was only performed quite recently by Kane.¹ He based his calculation on the fact that, at the L point, in the blende structure, $m_1 = m_2 > 0$ and $|m_3| \gg m_1$, where m_1 , m_2 , and m_3 are the principal effective masses. Kane used the adiabatic approximation to solve the Schrödinger equation of the exciton:

$$\left(\frac{p_1^2}{2m_1} + \frac{p_2^2}{2m_2} + \frac{p_3^2}{2m_3} - \frac{e^2}{Kr} \right) \Phi(r) = E \Phi(r), \quad (1)$$

where $\Phi(r)$ is the envelope function.

The imaginary part of dielectric constant ϵ_2 is written

$$\epsilon_2 = \frac{4\pi^2 e^2}{3m^2 \omega^2 V} \sum_f |P_{if}|^2 \delta(E_f - E_i - \hbar\omega), \quad (2)$$

where

$$P_{if} = \langle U_i | P | U_f \rangle \Phi(0) \sqrt{V}$$

is the matrix element of momentum between initial

and final states, U_i and U_f are the cell periodic parts of the Bloch function at critical point, and V is the volume.

Following Kane's calculation, Eq. (2) can be written

$$\epsilon_2(\omega) = 8\pi^2 \frac{(m_{r1}/m_0)^2 \langle P^2 \rangle_{av}}{3m_0^2 a_0^2 K_\infty} N \frac{S_{tot}}{\omega^2}, \quad (3)$$

where a_0 is Bohr radius, $N=4$ is number of critical points, $\langle P^2 \rangle_{av} = 3 \langle P_x^2 \rangle_{av} = P^2$, K_∞ is the dielectric constant, m_{r1} is the reduced mass, and $S_{tot}(\omega)$ is a function taking into account the continuum structure and the structure associated with the two-dimensional bound state. The peak is asymmetric and drops sharply on the high-energy side.

In Fig. 1 we have plotted the reflectivity curves⁶ of CdTe, ZnTe, ZnSe, and HgTe, in the region of

$\Lambda_{4v}, \Lambda_{5v} \rightarrow \Lambda_{6c}$ transition,

$\Lambda_{6v} \rightarrow \Lambda_{6c}$ transition.

These curves were obtained with the sample temperature at 10°K by an apparatus described previously.⁷ The excitonic peaks and the structure of the critical point are clearly seen for CdTe and ZnTe. However, we do not observe the critical-point

structure for ZnSe and HgTe.

CdTe

We have calculated ϵ_2 by the Kramers-Kronig relations [Fig. 2(a)]. In order to isolate the contribution from one of the spin-orbit split bands, we assume⁸ that both bands give contributions of the same shape and amplitude, but shifted by 0.57 eV. Thus $\epsilon_2(\omega)$ has the form

$$\begin{aligned}\epsilon_2(\omega) &= 3.5 + \epsilon'_2(\omega) + \epsilon'_2(\omega - \Delta_1), \\ \epsilon'_2(\omega) &= 0 \text{ if } \hbar\omega \leq 2.60 \text{ eV.}\end{aligned}\quad (4)$$

Using the values of the different parameters occurring in Eq. (3) (see Table I), we calculate⁹

$$\epsilon'_2 = 6.3 S_{\text{tot}} \text{ near } 3.5 \text{ eV.} \quad (5)$$

We have taken our energy zero and zero for S_{tot} to coincide; the experimental amplitude of ϵ'_2 is 8.5:

$$S_{\text{tot}} = 1.35. \quad (6)$$

This corresponds to $|m_3/m_1| = 28$.

In Fig. 2(b) the solid curve is $\epsilon'_2(\omega)$; the theoretical curve (dashed) was computed for mass ratio -40 . The amplitudes were scaled to make the peaks agree; we see that the energy scale agrees very well. The theoretical binding energy is

$$E_B^{\text{th}} = \frac{1}{2(n + \frac{1}{2})^2} \frac{m_{r\perp}}{m_0} \frac{e^4}{\hbar^2 K_\infty^2} \approx 2 \frac{m_{r\perp}}{m_0} \frac{e^4}{\hbar^2 K_\infty^2} = 0.16 \text{ eV}$$

because the term $n=0$ contains 95% of the oscillator strength, and the experimental value is 0.15 eV.

Thus, in spite of the fact that the lifetime broad-

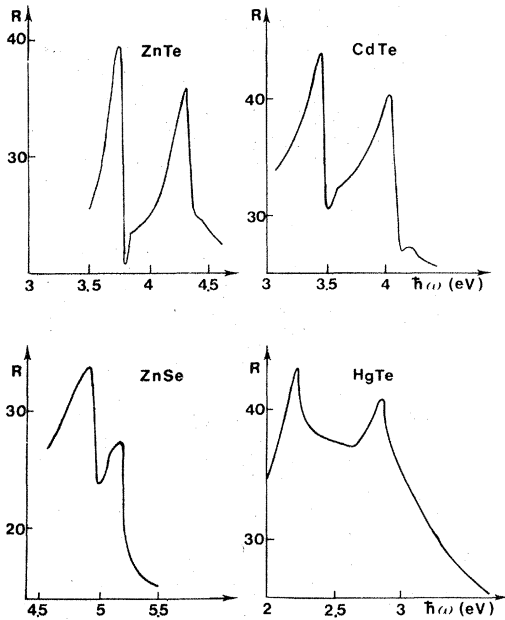


FIG. 1. Reflectivity curves for ZnTe, CdTe, ZnSe, HgTe at 10°K.

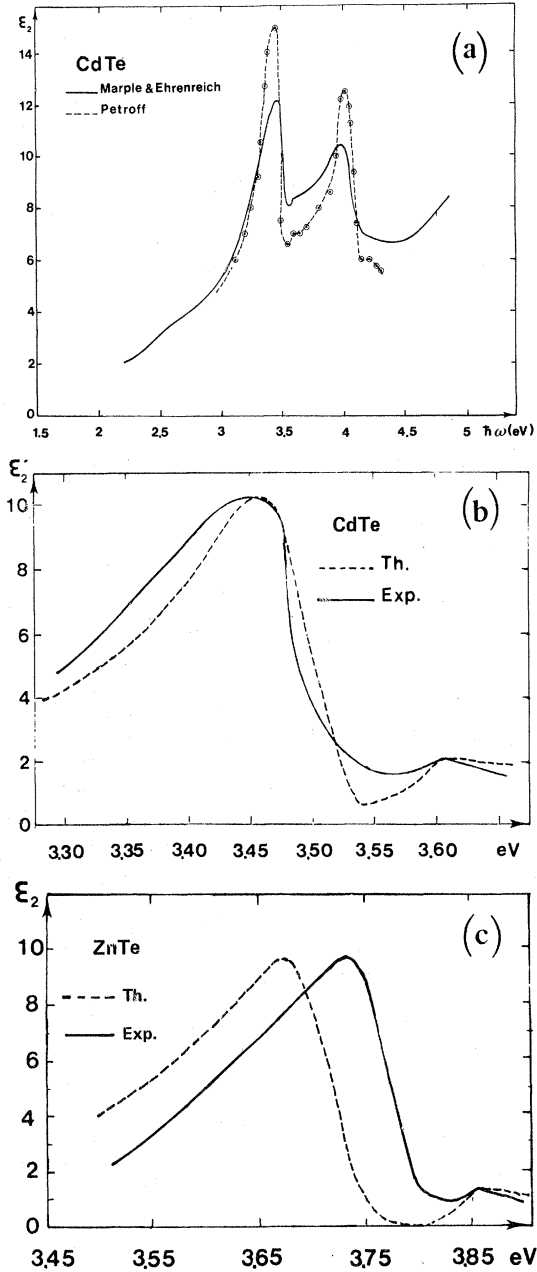


FIG. 2. (a) Imaginary part of dielectric constant ϵ_2 in CdTe. (b) The solid curve is $\epsilon'_2(\omega)$ —the contribution of one of the spin-orbit components to ϵ_2 in CdTe; the dashed line is theoretical curve computed for $|m_3/m_1| = 40$. (c) The solid curve is $\epsilon'_2(\omega)$ —the contribution of one of the spin-orbit components to ϵ_2 in ZnTe; the dashed line is theoretical curve computed for $|m_3/m_1| = 40$.

ening is not included in the theory, the agreement between experiment and theory is quite satisfactory; however, the value of $|m_3/m_1| = 28$ is twice as strong as that obtained by Kane.⁹

Figure 2(a) also shows the results of a previous experiment in CdTe.¹⁰ The discrepancy between the

TABLE I. Numerical parameters which have been used for the calculation of ϵ_2 .

	P^2 (a. u.)	E_{G_1} (eV)	Δ_1 (eV)	K_∞	$m_{r\perp}$	E_B^{th} (eV)
CdTe	0.31 ^a	3.61 ^b	0.57 ^b	7.05 ^c	0.149 m_0 ^d	0.16
ZnTe	0.24 ^a	3.86 ^b	0.57 ^b	7.28 ^e	0.204 m_0 ^d	0.20
ZnSe	0.26 ^a	?	0.29 ^b	6.1 ^f	0.245 m_0 ^d	0.3
HgTe	0.21 ^a	?	0.62 ^b			

^aCalculated by taking a three-band formula

$$\frac{1}{m_c^*} = \frac{1}{m_0} + \frac{2\hbar^2}{m_0^2} \left(\frac{2}{3} \frac{P^2}{E_{G_0}} + \frac{1}{3} \frac{P^2}{E_{G_0} + \Delta_0} \right).$$

^bOur experimental results at 10°K.^cK. K. Kanazawa and F. C. Brown, Phys. Rev. **135A**, 1757 (1964).^dCalculated by three-band formula

$$\frac{1}{m_{cl}} = \frac{1}{m_0} + \frac{\hbar^2 P^2}{m_0^2} \left(\frac{1}{E_{G_1}} + \frac{1}{E_{G_1} + \Delta_1} \right),$$

$$\frac{1}{m_{vl}} = \frac{1}{m_0} + \frac{\hbar^2 P^2}{m_0^2} \left(-\frac{1}{E_{G_1}} \right).$$

^eR. Le Toullec, Ph. D. dissertation, Paris, 1968 (unpublished).^fS. S. Mitra, J. Phys. Soc. Japan Suppl. **21**, 61 (1966).

two experimental results [see Fig. 2(a)] may arise from two sources: (i) pollution of the sample at low temperature—to avoid this, we work in a vacuum of 10^{-9} mm of Hg; and (ii) the limiting conditions of the Kramers-Kronig transformation.

We do not know of any direct theoretical calculation of m_3 and m_1 on the II-VI compounds; however, we can compare our results to the value $|m_3/m_1| \approx 11$ obtained for InSb¹¹ by the $\vec{K} \cdot \vec{P}$ method.

ZnTe

Using a similar analysis for ZnTe, we have adopted the function

$$\epsilon_2(\omega) = \epsilon_2'(\omega) + \epsilon_2''(\omega - \Delta_1) + 2.40, \quad (7)$$

$$\epsilon_2'(\omega) = 0 \quad \text{if } \hbar\omega \leq 3.20 \text{ eV};$$

using values taken from Table I we find

$$\epsilon_2' = 7.7S_{\text{tot}} \quad \text{near } 3.75 \text{ eV}. \quad (8)$$

The height of the peak of $\epsilon_2'(\omega)$ [Fig. 2(c)] is 8.25, from which we conclude that

$$S_{\text{tot}} = 1.07,$$

which corresponds to $|m_3/m_1| = 20$.

While there is agreement between the shape of the theoretical and experimental curves, there is a significant energy shift between the two peaks

$$E_B^{\text{th}} = 0.20 \text{ eV} \quad \text{and} \quad E_B^{\text{exp}} = 0.11 \text{ eV}.$$

The experimental value of the binding energy is weaker than the theoretical value. However the band structure of ZnTe is very similar to that of CdTe, and from the relatively large ratio of the effective masses $|m_3/m_1| = 20$, the adiabatic approximation is still valid.

ZnSe

We were not able to determine the binding energy and the ratio m_3/m_1 for ZnSe because it is not possible to see the critical point (Fig. 1). This can be explained by the fact that the spin-orbit splitting $\Delta_1 = 0.29$ eV is nearly equal to the binding energy of the exciton. Thus the structure of the critical point is overlapped by the exciton peak associated to the transition $L_{6u} \rightarrow L_{6c}$.

None of the preceding effects were observed for HgTe, probably because of the low binding energy $E_B^{\text{th}} = 0.04$, which is much too small (as in III-V compounds) to be resolved in these experiments.

For the four compounds studied, we have used the high-frequency dielectric constant K_∞ ; this is justified by the fact that

$$a_{ex} < (\hbar/m_{r\perp}\omega_0)^{1/2},$$

where a_{ex} is the radius of the exciton orbit and ω_0 the optical mode vibrational frequency. The value of $a_{ex} = (K_\infty/m_{r\perp})a_0$ is 25 Å for CdTe, 19 Å for ZnTe, and 13 Å for ZnSe, and $(\hbar/m_{r\perp}\omega_0)^{1/2} \approx 120$ Å.

In conclusion, it seems that the Kane model applies well to the II-VI compounds. However, we can observe that the agreement between the theory and experiment decreases in going from CdTe to ZnTe and to ZnSe. This corresponds to a decreasing of the radius of the exciton orbit and in the limiting case of ZnSe the Wannier exciton model may no longer hold.

ACKNOWLEDGMENTS

We wish to thank E. O. Kane and M. L. Cohen for stimulating discussions.

¹E. O. Kane, Phys. Rev. **180**, 852 (1969).²M. Cardona and G. Harbeke, Phys. Rev. Letters **8**, 90 (1962).³J. C. Phillips, Phys. Rev. **136A**, 1705 (1964).⁴C. B. Duke and B. Segall, Phys. Rev. Letters **17**, 19 (1966).⁵B. Velicky and J. Sak, Phys. Status Solidi **16**, 147 (1966).⁶J. P. Walter, M. L. Cohen, Y. Petroff, and M.Balkanski, Phys. Rev. B **1**, 2661 (1970) for ZnSe, ZnTe; *ibid.* (to be published) for CdTe, HgTe.⁷Y. Petroff, R. Pinchaux, J. Dagheaux, and M. Balkanski, Rev. Phys. Appl. (to be published).⁸The authors would like to thank Dr. Kane for providing the details of his calculation.⁹The original paper reported a numerical coefficient of 2.1. E. O. Kane, Phys. Rev. B **2**, 4305 (1970).¹⁰D. T. F. Marple and H. Ehrenreich, Phys. Rev.

Letters 8, 87 (1962).

¹¹C. W. Higginbotham, F. H. Pollak, and M. Cardona, in

Proceedings of the Ninth International Conference on Physics of Semiconductors (Nauka, Leningrad, 1968), Vol. I, p.57.

PHYSICAL REVIEW B

VOLUME 3, NUMBER 10

15 MAY 1971

Brillouin-Scattering Analysis of Phonon Interactions in Acoustoelectric Domains in GaAs†

E. D. Palik* and Ralph Bray

Physics Department, Purdue University, Lafayette, Indiana 47907

(Received 29 June 1970)

Acoustoelectrically amplified domains of ultrasonic flux in GaAs were used for analyses of various phonon interactions by Brillouin-scattering techniques. Both the growth of the flux from the thermal equilibrium phonon spectrum and particularly the attenuation (after the amplifying voltage pulse was shut off) were studied as a function of ultrasonic frequency in the broad range from 0.3 to 4.0 GHz at 300 °K. The data were analyzed to give the magnitude and frequency dependence of both the acoustoelectric gain and the lattice attenuation in the weak-flux regime. Comparison with small-signal gain theory in the $ql \approx 1$ range, for piezoelectrically active [110] shear waves, gave good agreement. The lattice attenuation was determined not only for the amplified shear waves but also for the piezoelectrically inactive longitudinal waves, which were obtained by mode conversion upon reflection of the amplified shear-wave domain. The frequency dependence of the attenuation, proportional to $f^{1.8}$ and $f^{1.3}$, respectively, fell well below the expected f^2 behavior. In the strong-flux regime, striking anomalous attention was found, consisting of a too-rapid initial attenuation of low frequencies, and too-slow initial attenuation of higher frequencies. These results are interpreted to represent a dominant trend of up-conversion of intense ultrasonic flux from low to high frequencies by nonlinear frequency-mixing processes. Evidence is summarized favoring such frequency-mixing processes, over possible variation in the frequency dependence of the acoustoelectric gain in strong flux, as a dominant factor in the evolution of the strong-flux spectrum both in growth and attenuation.

I. INTRODUCTION

Domains of intense acoustic flux, containing a rather broad band of frequencies in the low-GHz range, can be produced in piezoelectric semiconductors by acoustoelectric amplification of phonons from the thermal equilibrium spectrum.^{1,2} By means of Brillouin-scattering techniques,² it is possible to use such domains to follow the growth and attenuation of the various frequency components of the amplified acoustic flux and thus study various types of phonon interactions as a function of phonon frequency and intensity. Those studied in some detail in the present work include (a) the acoustoelectric interaction,³ a term applied here in the restricted sense of referring only to the exchange of energy and momentum between the electrons and the beam of amplified phonons, (b) the ordinary lattice attenuation of the amplified flux via the nonelectronic interaction with the thermal phonons of the lattice, and (c) phonon-phonon interactions of electronic origin which are a nonlinear extension⁴⁻⁶ of the acoustoelectric interaction and arise from the interaction of bunched electrons of one frequency with the piezoelectric fields associated with other frequencies. The resulting nonlinear mixing of frequencies and parametric inter-

actions cause up- and down-conversion in the frequencies of the acoustoelectrically amplified flux.

In analyzing these phonon interactions, we are faced with two problems: In general, the interactions coexist, making it necessary to devise methods of distinguishing them from one another; and the interactions are, in different degree, dependent on the intensity and spectral composition of the amplified flux. In sufficiently weak flux, where only the small-signal acoustoelectric and lattice-attenuation processes are present, these interactions can be separated fairly easily by making growth or attenuation measurements under variable current conditions, since only the acoustoelectric interaction is current dependent. The analysis becomes much more difficult in strong flux where deviations of the growth and attenuation from small-signal theory become evident. A most important observation there is the rapid shift and continued evolution of the spectral distribution of the amplified acoustic flux as it continues to grow.^{2,7} The problem of interpretation boils down to distinguishing between (i) a shift in the frequency dependence of the acoustoelectric interaction in strong flux and (ii) the onset of mixing and frequency conversion of the acoustic flux via interaction (c) above.

Our investigation of these problems was restricted